HEPATOLOGY
Official Journal of the American Association for the Study of Liver Diseases

CD73 (Ecto-5′-Nucleotidase) Hepatocyte Levels Differ Across Mouse Strains and Contribute to Mallory-Denk Body Formation

Natasha T. Snider,[1] Nicholas W. Griggs,[1] Amika Singla,[1] David S. Moons,[2] Sujith V.W. Weerasinghe,[1] Anna S. Lok,[3] Chunhai Ruan,[3] Charles F. Burant,[1,3] Hari S. Conjeevaram,[3] and M. Bishr Omary[1,3,4]

Formation of hepatocyte Mallory-Denk bodies (MDBs), which are aggregates of keratins 8 and 18 (K8/K18), ubiquitin, and the ubiquitin-binding protein, p62, has a genetic predisposition component in humans and mice. We tested the hypothesis that metabolomic profiling of MDB-susceptible C57BL and MDB-resistant C3H mouse strains can illuminate MDB-associated pathways. Using both targeted and unbiased metabolomic analyses, we demonstrated significant differences in intermediates of purine metabolism. Further analysis revealed that C3H and C57BL livers differ significantly in messenger RNA (mRNA) level, protein expression, and enzymatic activity of the adenosine-generating enzyme, ecto-5′-nucleotidase (CD73), which was significantly lower in C57BL livers. CD73 mRNA levels were also dramatically decreased in human liver biopsies from hepatitis C and nonalcoholic fatty liver disease patients. Feeding mice with a diet containing the MDB-inducing agent, 3,5-diethoxycarbonyl-1,4-dihydrocollidine (DDC), significantly decreased CD73 protein and activity in C57BL livers and resulted in loss of plasma membrane CD73 expression and activity in isolated mouse hepatocytes. To further examine the role of CD73 in MDB formation *in vivo*, we fed wild-type (WT) and CD73$^{-/-}$ mice a DDC-containing diet. Liver enlargement, p62 induction, and disappearance of the K8/K18 cytoskeleton were attenuated in CD73$^{-/-}$, compared to WT livers. MDB formation, as assessed by biochemical and immunofluorescence detection of keratin and ubiquitin complexes, was nearly absent in CD73$^{-/-}$ mice. *Conclusion*: Purine metabolism and CD73 expression are linked to susceptibility to MDB formation in livers of different mouse strains. Expression of the adenosine-generating enzyme, CD73, contributes to experimental MDB induction and is highly regulated in MDB-associated liver injury in mice and in chronic human liver disease. (HEPATOLOGY 2013;58:1790-1800)

Mallory-Denk bodies (MDBs) are intracellular aggregates of hepatocytes that contain the cytoskeletal intermediate filament proteins, keratins 8 and 18 (K8/K18), as their major components, in addition to ubiquitin, and the ubiquitin-binding protein, p62.[1] Cross-linking of keratins, particularly K8, by transglutaminase 2 (TG2) is critical for MDB formation.[2,3] MDBs are frequently observed alongside hepatocyte ballooning and loss of the cytoplasmic K8/K18 intermediate filament network.[4] Livers of patients with alcoholic and nonalcoholic steatohepatitis most frequently display MDBs as part of their pathology,[5] where

Abbreviations: Ab, antibody; AMP, adenosine monophosphate; ATP, adenosine triphosphate; cDNA, complementary DNA; CXCL10, C-X-C motif chemokine 10; DAPI, 4′,6-diamidino-2-phenylindole; DDC, 3,5-diethoxycarbonyl-1,4-dihydrocollidine; ECs, endothelial cells; GAPDH, glyceraldehyde-3-phosphate dehydrogenase; GMP, guanosine monophosphate; IF, immunofluorescence; IFN-γ, interferon-gamma; HCV, hepatitis C virus; H&E, hematoxylin and eosin; K8, keratin 8; KO, knockout; MDB, Mallory-Denk body; mRNA, messenger RNA; NAFLD, nonalcoholic fatty liver disease; NDPK, nucleoside diphosphate kinase; nt, nucleotide; qPCR, quantitative real-time polymerase chain reaction; RIPA, radioimmunoprecipitation; SDS-PAGE, sodium dodecyl sulfate/polyacrylamide gel electrophoresis; TCA, tricarboxylic acid; TG2, transglutaminase 2; TM, Tris-maleate buffer; WT, wild type.

From the Departments of [1]Molecular & Integrative Physiology, [2]Pathology, and [3]Medicine, University of Michigan Medical School, Ann Arbor, MI; and the [4]VA Ann Arbor Healthcare System, Ann Arbor, MI.

Received January 14, 2013; accepted May 10, 2013.

This work was supported by the National Institutes of Health (grant nos.: R01 DK52951 [to M.B.O.] and K01 DK093776 [to N.T.S.]) and Department of Veterans Affairs Merit Review Award (to M.B.O.). This work utilized Core Services (supported by NIH grant nos.: DK089503 and DK034933; to the University of Michigan).

MDB presence correlates with less-favorable outcomes.[6,7] MDBs are also observed in the context of hepatocellular carcinoma, viral hepatitis, and some forms of drug-induced liver injury.[1,8] However, MDBs are not observed in all patients with the same liver disease,[9,10] and increases in their formation over time are associated with decompensation and progression to cirrhosis in patients with hepatitis C virus (HCV) infection.[11] Identification of the factors that regulate or contribute to MDB formation may yield important insights into the general role of protein aggregation in liver disease pathogenesis.

Different strains of mice exhibit varying susceptibility to experimental MDB induction upon administration of the porphyrogenic compound, 3,5-diethoxycarbonyl-1,4-dihydrocollidine (DDC),[12] a long-standing model reflective of the major biochemical and ultrastructural features of human MDBs.[1] These strain differences are a useful paradigm for uncovering contributing factors to protein aggregation in hepatocytes, beyond the already known roles for protein misfolding and proteasomal inhibition.[13,14] Comparison of MDB-susceptible (C57BL) to MDB-resistant (C3H) mice at the proteomic level revealed major differences in the energy metabolism and oxidative-stress-sensitive enzymes, glyceraldehyde-3-phosphate dehydrogenase (GAPDH) and nucleoside diphosphate kinase (NDPK).[15] Given the critical housekeeping functions of GAPDH in glycolysis and NDPK in nucleotide (nt) metabolism, we hypothesized that these two strains also exhibit differences in their liver metabolomes that may ultimately affect their response to liver injury caused by DDC.

In the present study, we performed both targeted and unbiased metabolomic analyses to compare C3H and C57BL mouse livers, which ultimately led us to identify ecto-5′-nucleotidase (CD73) as a modulator of MDB formation in mouse liver. CD73 is a glycosylphosphatidylinositol-linked, membrane-bound glycoprotein that catalyzes the phosphohydrolysis of adenosine 5′-monophosphate (AMP) to form adenosine.[16] As the major source of extracellular adenosine, CD73 controls important physiological responses in inflammation, epithelial transport, tissue barrier function, and hypoxia, among others.[16,17] Based on *in vivo* data using $CD73^{-/-}$ mice, it was previously demonstrated that CD73 contributes to ethanol-induced liver steatosis[18] and thioacetamide- or CCL_4-induced liver fibrosis.[19] Using *ex vivo* and *in vivo* approaches, we demonstrate that C3H and C57BL mice have differences in expression and regulation of CD73 during liver injury and that CD73 contributes to MDB formation in mice.

Materials and Methods

Antibodies. The following antibodies (Abs) were used: rat anti-CD73 (R&D Systems, Minneapolis, MN) for immunoblotting; anti-CD73 (TY/23; BD Bioscience, San Jose, CA) for immunofluoresence (IF) staining; anti-K8 Troma I (Developmental Studies Hybridoma Bank, Iowa City, IA); anti-K8/K18 rabbit Ab 8592 for IF staining of mouse K8/K18[20]; anti-DDK (Flag; OriGene Technologies, Inc., Rockville, MD); mouse anti-Ub and goat anti-p62 (Santa Cruz Biotechnology, Santa Cruz, CA); rabbit anti-transglutaminase 2 (TG2; Thermo Fisher Scientific Inc., Waltham, MA); and rabbit anti-EEA1, anti-PDI, anti-RCAS1, and anti-LAMP1 (Cell Signaling Technology, Danvers, MA) for immunostaining of organelle markers.

Quantitative Polymerase Chain Reaction. RNA extraction, quantitative real-time polymerase chain reaction (qPCR), and data analysis were performed as previously described[15] using human and mouse gene-specific primers (Supporting Table 1).

Human and Animal Liver Experiments. Human liver specimens were biopsies from HCV and nonalcoholic fatty liver disease (NAFLD) patients collected at the University of Michigan (Ann Arbor, MI) under an approved human subjects protocol. Information on pathology findings is provided in Supporting Table 2. MDB induction experiments in C3H/He (C3H) and C57BL/6J (C57BL) mice were done as previously described.[12] $CD73^{-/-}$ mice in a C57BL background[21] were provided by Dr. Linda Thompson (Oklahoma Medical Research Foundation, Oklahoma City, OK). Age- and sex-matched wild-type (WT) C57BL and $CD73^{-/-}$ mice were used (2 control and 9 DDC-fed mice [4 animals for 3 weeks and 5 animals for 3 months]) in the DDC experiment that was performed

Address reprint requests to: Natasha Snider, Ph.D., Department of Molecular & Integrative Physiology, University of Michigan Medical School, 7720 Medical Science II, 1301 East Catherine Street, Ann Arbor, MI 48109-5622. E-mail: nsnider@umich.edu; fax: 734-936-8813.

Copyright © 2013 by the American Association for the Study of Liver Diseases.

View this article online at wileyonlinelibrary.com.

DOI 10.1002/hep.26525

Potential conflict of interest: Nothing to report.

Additional Supporting Information may be found in the online version of this article.

in duplicate, and as previously described.[12] For metabolomic analysis (3 mice/strain), mice were fasted for 5 hours, after which they were sacrificed and their livers rapidly excised and snap-frozen. The left liver lobe from each mouse was used in the metabolomic analysis (see below). All mice received humane care and their use was approved by, and performed in accord with, the university committee on use and care of animals at the University of Michigan.

Metabolomics. Metabolomic analysis was performed at the Michigan Regional Comprehensive Metabolomics Resource Core (University of Michigan). Pulverized mouse liver tissues were extracted with a methanol, acetone, and acetonitrile mixture (1:1:1). For liquid chromatography/mass spectrometry analysis of metabolites, samples were separated using an Agilent 1200 analytical HPLC on a Luna NH2 HILIC column, followed by injection into the mass spectrometer (Agilent 6410 series triple quadrupole with electrospray ionization source; Agilent Technologies, Inc., Santa Clara, CA), which was operated in negative mode. Data were processed by MassHunter workstation software (version B.04; Agilent).

Preparation of Tissue Lysates and Immunoblotting. Total liver homogenates were prepared by homogenizing tissues in 2× sample buffer (4% sodium dodecyl sulfate [SDS], 10% 2-mercaptoethanol, 20% glycerol, 0.004% bromophenol blue, and 0.125 M of Tris-HCl; pH 6.8). Total lysates were used in immunoblottings for TG2, p62, K8, and ubiquitin. For radioimmunoprecipitation (RIPA) buffer lysates (used in CD73 immunoblotting and enzyme activity), livers were homogenized in ice-cold RIPA buffer (150 mM of sodium chloride, 1% NP-40, 0.5% sodium deoxycholate, 0.1% SDS, and 50 mM of Tris; pH 8) with protease inhibitors. Lysates were resolved on gradient 4%-20% SDS-PAGE (polyacrylamide gel electrophoresis) gels, then transferred onto polyvinylidene difluoride membranes, which were subsequently blocked (5% milk in phosphate-buffered saline and 0.1% Tween-20) and incubated with the designated Abs.

Biochemical Measurement of CD73 Enzymatic Activity. CD73 activity was measured in mouse liver RIPA lysates using a kit (BQ Kits, San Diego, CA). The assay was based on a four-reaction sequence, beginning with hydrolysis of 5′-inosine monophosphate to form inosine and ending with the generation of a quinone dye from hydrogen peroxide (by-product of uric acid synthesis), which was monitored spectrophotometrically in a time-dependent manner. The assay's specificity for CD73, under our experimental conditions, was verified using $CD73^{-/-}$ liver lysate controls.

CD73 Enzyme Histochemistry. CD73 activity in fixed hepatocytes and tissue sections (6 μm) was done using a modified version of a published protocol.[22] Cells and tissue sections were fixed in 10% neutral buffered formalin for 5 minutes at 4°C, rinsed in 0.1 M of Tris-maleate (TM) buffer (pH 7.2), then incubated in reaction medium (1 hour at 37°C). Reaction medium was prepared by first dissolving magnesium chloride (10 mM) and lead nitrate (3.6 mM) in TM buffer at 50°C until the solution became clear, then cooled to 37°C. Tissue-nonspecific alkaline phosphatase inhibitor (levamisole; 5 mM) and substrate (AMP; 1 mM) were added before incubation. After incubation, reactions were stopped by several rinses with water, followed by 1-minute incubation in sodium sulfide (1% w/v) and mounting in Prolong Gold reagent with 4′,6-diamidino-2-phenylindole (DAPI).

IF Staining and Confocal Imaging. After acetone fixation (10 minutes, −20°C), 6-μm-thick tissue sections were stained as previously described.[15] CD73 complementary DNA (cDNA) in pCMV6-Entry vector was purchased from OriGene Technologies. Primary hepatocytes were isolated and transfected as described previously.[15] Hepatocytes were transfected with CD73 for 24 hours, followed by a 24-hour treatment with DDC (100 μM), then fixed in methanol (10 minutes, −20°C) before immunostaining.

Results

Metabolomic Analysis of Livers From C3H and C57BL Mice. We initially performed a targeted analysis for metabolic intermediates of glycolysis, tricarboxylic acid (TCA) cycle, and nucleotide metabolism in untreated C3H and C57BL mice (Table 1). The graph data were presented and statistically analyzed using Prism 5 software (GraphPad Software). Of the 21 metabolites assayed, adenosine triphosphate (ATP) and guanosine monophosphate (GMP) showed statistically significant differences ($P < 0.05$). We also performed an unbiased analysis, which revealed differences in several amino acids, carbohydrates, vitamins, and lipids (Supporting Table 3), in addition to nucleotide intermediates. Significant differences in the nucleobase adenine (C3H<C57BL) and the nucleoside inosine (C3H>C57BL) were observed (Fig. 1A). Based on these findings, we focused on the ATP branch of the purine-metabolism pathway (Fig. 1B) for further validation and mechanistic analysis.

We asked whether the two strains have differences in the expression of enzymes involved in purine nucleotide synthesis, metabolism, and salvage. Although

Table 1. Metabolomic Comparison of Nucleotides, Glycosis, and TCA Cycle Intermediates in C3H and C57BL Livers

Metabolite	C3H (nmol/mg Liver Tissue)	C57BL (nmol/mg Liver Tissue)	*P* Value
LAC	4.7 ± 0.2	3.4 ± 0.9	0.23
MAL	0.0012 ± 0.0002	0.0014 ± 0.0003	0.56
FUM	0.12 ± 0.06	0.16 ± 0.03	0.56
F6P/G6P	0.20 ± 0.01	0.20 ± 0.02	1.00
CIT/ICIT	0.16 ± 0.004	0.14 ± 0.02	0.35
Pyr	0.21 ± 0.01	0.19 ± 0.02	0.43
2PG/3PG	0.026 ± 0.003	0.019 ± 0.003	0.15
aCoA	0.021 ± 0.006	0.020 ± 0.004	0.91
PEP	0.0065 ± 0.002	0.0032 ± 0.0006	0.21
FBP	0.024 ± 0.02	0.0056 ± 0.004	0.32
FAD	0.068 ± 0.002	0.068 ± 0.002	0.87
NAD	0.32 ± 0.004	0.36 ± 0.02	0.16
NADH	0.32 ± 0.01	0.37 ± 0.02	0.08
NADP	0.052 ± 0.005	0.056 ± 0.003	0.46
NADPH	0.34 ± 0.3	0.42 ± 0.4	0.87
AMP	2.26 ± 0.009	2.6 ± 0.15	0.08
ADP	0.56 ± 0.02	0.58 ± 0.02	0.64
ATP	0.12 ± 0.003	0.10 ± 0.003*	0.02
GMP	0.33 ± 0.005	0.45 ± 0.03*	0.01
GDP	0.097 ± 0.05	0.037 ± 0.02	0.28
GTP	0.011 ± 0.009	0.0037 ± 0.003	0.46

Abbreviations: LAC, lactate; MAL, malate; FUM, fumarate; F6P, fructose 6-phosphate; G6P, glucose 6-phosphate; CIT, citrate; ICIT, isocitrate; Pyr, pyruvate; 2PG, 2-phosphoglycerate; 3PG, 3-phosphoglycerate; aCoA, acetyl coenzyme A; PEP, phosphoenolpyruvate; FBP, fructose 1,6-biphosphate; FAD, flavin adenine dinucleotide; NAD, nicotinamide adenine dinucleotide; NADH, nicotinamide adenine dinucleotide, reduced; NADP, nicotinamide adenine dinucleotide phosphate; NADPH, nicotinamide adenine dinucleotide phosphate, reduced; ADP, adenosine diphosphate; GDP, guanosine diphosphate; GTP, guanosine triphosphate.

there are numerous enzymes that can exert control over these pathways, the major ones are depicted in the simplified schematic shown in Fig. 1B. Comparison of messenger RNA (mRNA) levels showed significantly lower levels of CD73 and PNP in C57BL livers (Fig. 1C). Because CD73 is upstream of PNP and its mRNA in C57BL livers is only 25% of C3H livers, we chose to study it in more detail. Importantly, we found a striking decrease (<20% of control) in CD73 mRNA in human liver biopsies from patients with fibrosis resulting from HCV infection or NAFLD (Fig. 1D,E). This was in stark contrast to increases in the following reference genes: interferon-gamma (IFN-γ) and C-X-C motif chemokine 10 (CXCL10) in HCV[23] and fatty-acid-binding protein and collagen 1a1 in NAFLD.[24]

CD73 mRNA and Protein Are Markedly Higher in C3H, Compared to C57BL, Livers. Quantitative CD73 mRNA assessment revealed dramatically lower levels in C57BL livers (Fig. 2A), which was reflected in isolated hepatocytes (Fig. 2B) and paralleled by the protein levels in C57BL (but not C3H) livers, as assessed by immunoblotting of liver lysates (Fig. 2C) and IF analysis of liver sections (Fig. 2D). Furthermore, DDC diminished CD73 activity in C3H and C57BL livers, as measured by enzyme histochemistry and compared to $CD73^{-/-}$ livers as a control (Fig. 2E). Prominent porphyria was evident in both strains after DDC treatment (Fig. 2E, dark deposits highlighted by arrows). The increase in CD73 mRNA in C3H DDC livers without an increase at the protein and activity levels may be related to translational control or antibody reactivity masking.

CD73 protein expression was lost in isolated hepatocytes as early as 1 hour postisolation (Fig. 3A) and was still absent at 48 hours postisolation (not shown), regardless of the mouse strain. Therefore, to study the effects of DDC on CD73 *ex vivo*, we transfected C57BL hepatocytes with the cDNA of flag-tagged mouse CD73. After transfection, we detected a CD73 monomer (~68 kD) and a dimer (~140 kD; Fig. 3B), as expected, because endogenous CD73 exists as a dimer on the plasma membrane.[25] The ectopically expressed CD73 exhibited both plasma membrane and intracellular localization under normal conditions (Fig. 3C, left panel) and was enzymatically active (Fig. 3D). However, upon DDC treatment, CD73 was lost from the plasma membrane and accumulated in intracellular granules (Fig. 3C, right panel). Costaining with different organelle markers revealed partial colocalization with resident proteins of the endoplasmic reticulum, Golgi, and early endosomes, but not lysozomes (Supporting Fig. 1), suggesting that the ability of CD73 to proceed along the secretory pathway may be compromised in the presence of DDC. Furthermore, there was a complete loss of hepatocyte CD73 activity after DDC treatment (Fig. 3E), reflecting the *in vivo* data.

Comparison of DDC-Induced MDB Formation in WT and $CD73^{-/-}$ Mice. We assessed the effect of 3-week and 3-month DDC feeding in WT C57BL (referred to as WT hereafter) and $CD73^{-/-}$ (in the C57BL background) mice. DDC decreased CD73 activity in WT mice by ~60%, as measured in the detergent-soluble liver fractions using a biochemical approach, as described in Materials and Methods (Fig. 4A). Serum alanine aminotransferase levels after DDC were similarly elevated in WT and $CD73^{-/-}$ mice (Supporting Fig. 2A). WT mice exhibited a time-dependent increase in their liver/body-weight ratios (Fig. 4B), a well-established effect of DDC feeding that is the result of a combination of factors, such as hepatocyte ballooning, ductular reaction, and porphyria.[1,3,26] Although liver enlargement also occurred in DDC-treated $CD73^{-/-}$ mice, it was significantly less

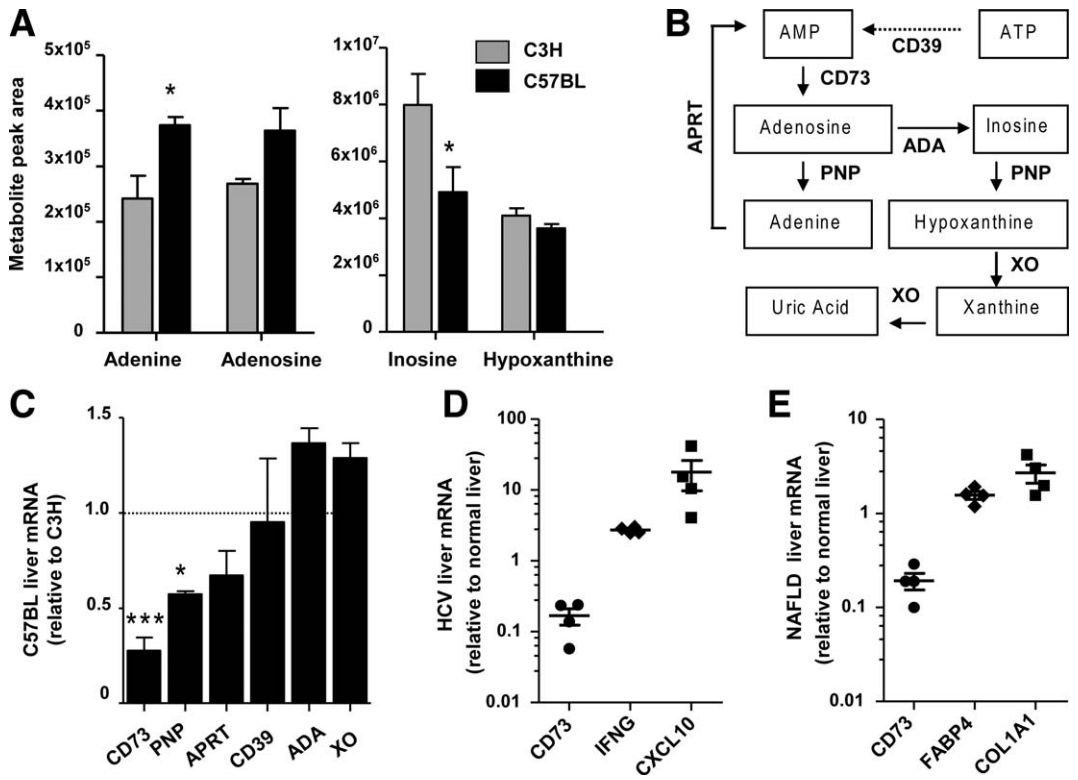

Fig. 1. Differences in substrates and enzymes of the purine-metabolism pathway in C3H and C57BL livers. (A) Measurement of nt metabolism intermediates using unbiased metabolomic analysis of the same C3H and C57BL livers as in Table 1 (n = 3 livers/strain). $*P < 0.05$, two-way analysis of variance. (B) Purine nt metabolites and the corresponding enzymes involved in their synthesis and metabolism. The ecto-apyrase, CD39, converts extracellular ATP to AMP, which is, in turn, converted to extracellular adenosine by the ecto-5′-nucleotidase, CD73. Intracellular adenosine is converted to either adenine by purine nt phosphorylase (PNP) or to inosine by adenosine deaminase (ADA). Adenine phosphoribosyltransferase (APRT) regenerates AMP from adenine. PNP generates hypoxanthine from inosine, whereas xanthine oxidase (XO) generates xanthine and uric acid. (C) Comparison of mRNA levels of purine nt metabolism enzymes. C57BL liver mRNA values are expressed as fold change relative to C3H livers. $*P < 0.05$; $***P < 0.001$; unpaired *t* test (C3H versus C57BL). (D and E) Measurement of CD73 mRNA levels in human HCV and NAFLD liver biopsies. Reference genes IFN-γ and CXCL10 (HCV) and FABP4 and COL1A1 (NAFLD) are shown as positive controls. Values are expressed as fold change (log scale) over normal liver biopsies (2 controls).

than WT mice after 3 months of DDC feeding (Fig. 4B). There were lower levels of the ubiquitin-binding (and MDB component) protein, p62, in $CD73^{-/-}$ livers after 3 months of DDC feeding (Fig. 4C). We found no evidence of CD73 and p62 colocalization in DDC-treated livers (Supporting Fig. 2B). TG2 was significantly up-regulated in both WT and $CD73^{-/-}$ mice (Fig. 4C) in response to injury. The limited p62 induction in $CD73^{-/-}$ livers after DDC feeding suggested that they may exhibit fewer MDBs, compared to WT mice. This was confirmed biochemically (Fig. 4D) by immunoblotting analysis for high-molecular-mass K8 and ubiquitin complexes that migrate near the top of the gel and represent cross-linked K8 and ubiquitin-containing species.[3] These complexes were present in WT, but largely absent from $CD73^{-/-}$, livers (Fig. 4D).

Ballooning degeneration in hepatocytes occurs with concomitant loss of the K8/K18 cytoskeleton.[4] There were no significant differences in K8/K18 between untreated $CD73^{-/-}$ mice, compared to untreated WT mice (Supporting Fig. 2C). On the other hand, after DDC treatment, there was a significant loss of the K8/K18 filament network in WT livers, but not in $CD73^{-/-}$ livers (Figure 5A). Histological analysis showed that, whereas both WT and $CD73^{-/-}$ mice displayed a significant response to DDC, including porphyria, hypertrophy, and bile stasis, there was significantly more cellular ballooning and steatosis present in WT, compared to the knockout (KO), livers (Fig. 5B and Supporting Fig. 2D). Furthermore, MDBs were mainly noted in WT livers (Fig. 5B, arrows). Because only large MDBs are observed by hematoxylin and eosin (H&E) staining,[1] we asked whether $CD73^{-/-}$ livers form smaller MDBs, only noted after IF analysis of keratin and ubiquitin-containing aggregates. As shown by the representative data in Fig. 6, such aggregates were only present in WT, but not $CD73^{-/-}$, livers (Fig. 6). Combined, these data demonstrate that CD73 is an important mouse-strain-related modulator of MDB formation.

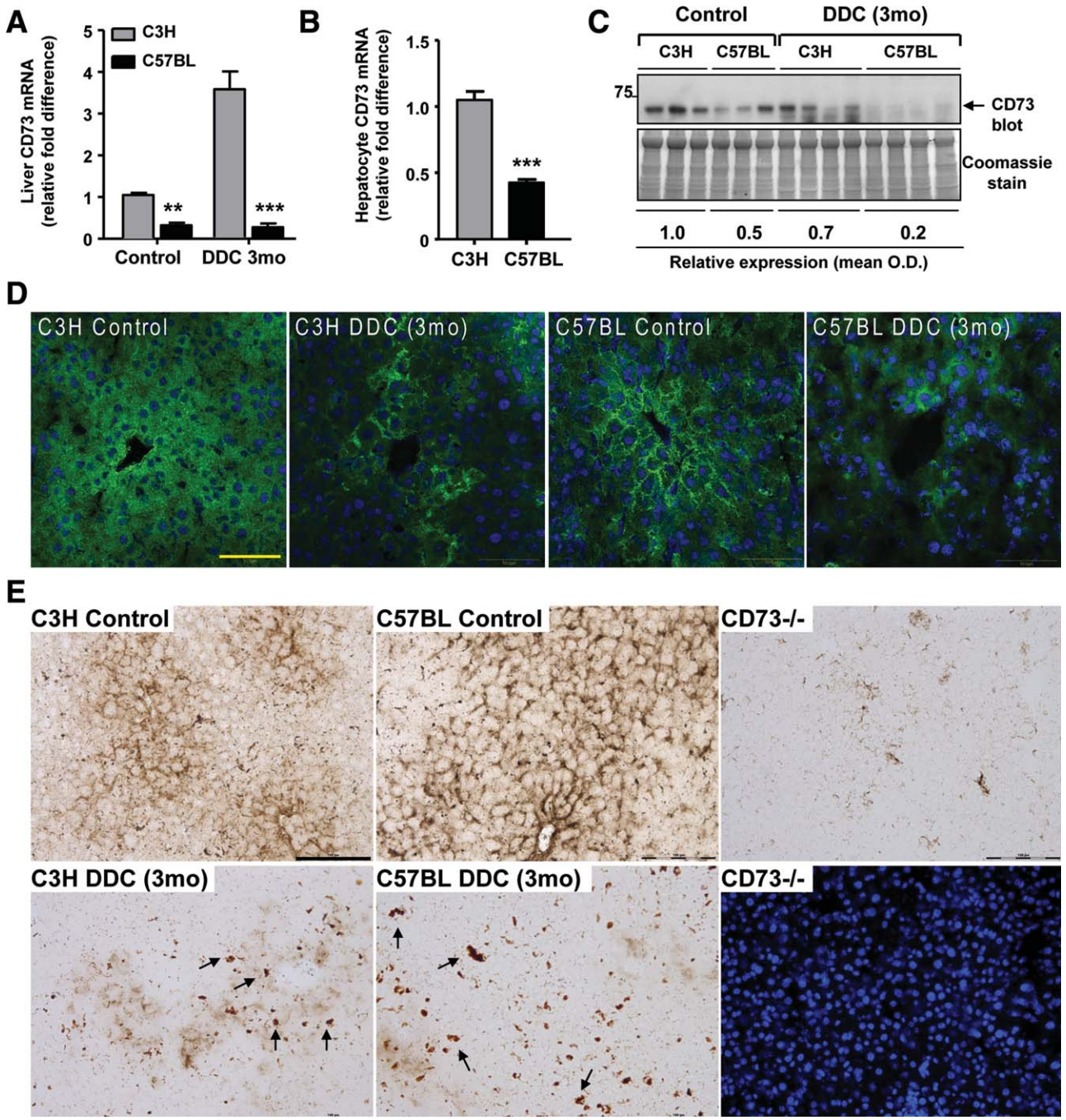

Fig. 2. Significantly decreased expression and activity of CD73 in C57BL mouse liver after DDC treatment. (A) Measurement of CD73 mRNA in C3H and C57BL livers from untreated (control) and DDC-treated (3 months) mice. Values are expressed as fold difference from C3H control livers. $^{**}P < 0.01$; $^{***}P < 0.001$; two-way analysis of variance. (B) Measurement of CD73 mRNA in isolated hepatocytes from C3H and C57BL mice. $^{***}P < 0.001$; unpaired *t* test. (C) CD73 immunoblotting of liver lysates from C3H and C57BL livers from untreated (control) and DDC-treated (3 months) mice. Relative expression values are averaged for the 3 control and 4 DDC livers per strain and normalized to C3H control livers. O.D. = optical density. (D) IF detection of CD73 protein (green) with DAPI nuclei (blue) in C3H and C57BL livers from control and DDC-treated (3 months) mice. Scale bar = 50 μm. (E) AMPase activity in control and DDC-treated (3 months) C3H and C57BL livers. A loss of CD73 enzymatic activity and porphyrin accumulation (arrows highlight porphyrin deposits) are observed after DDC treatment. $CD73^{-/-}$ AMPase activity is shown, together with the corresponding DAPI-stained nuclei, as a negative control. Scale bar = 100 μm.

Discussion

We initiated our present study with a global approach to examine differences in metabolic pathways between MDB-susceptible and -resistant mice. The results from the metabolomic assessment led us to focus on the purine-metabolism pathway, from which

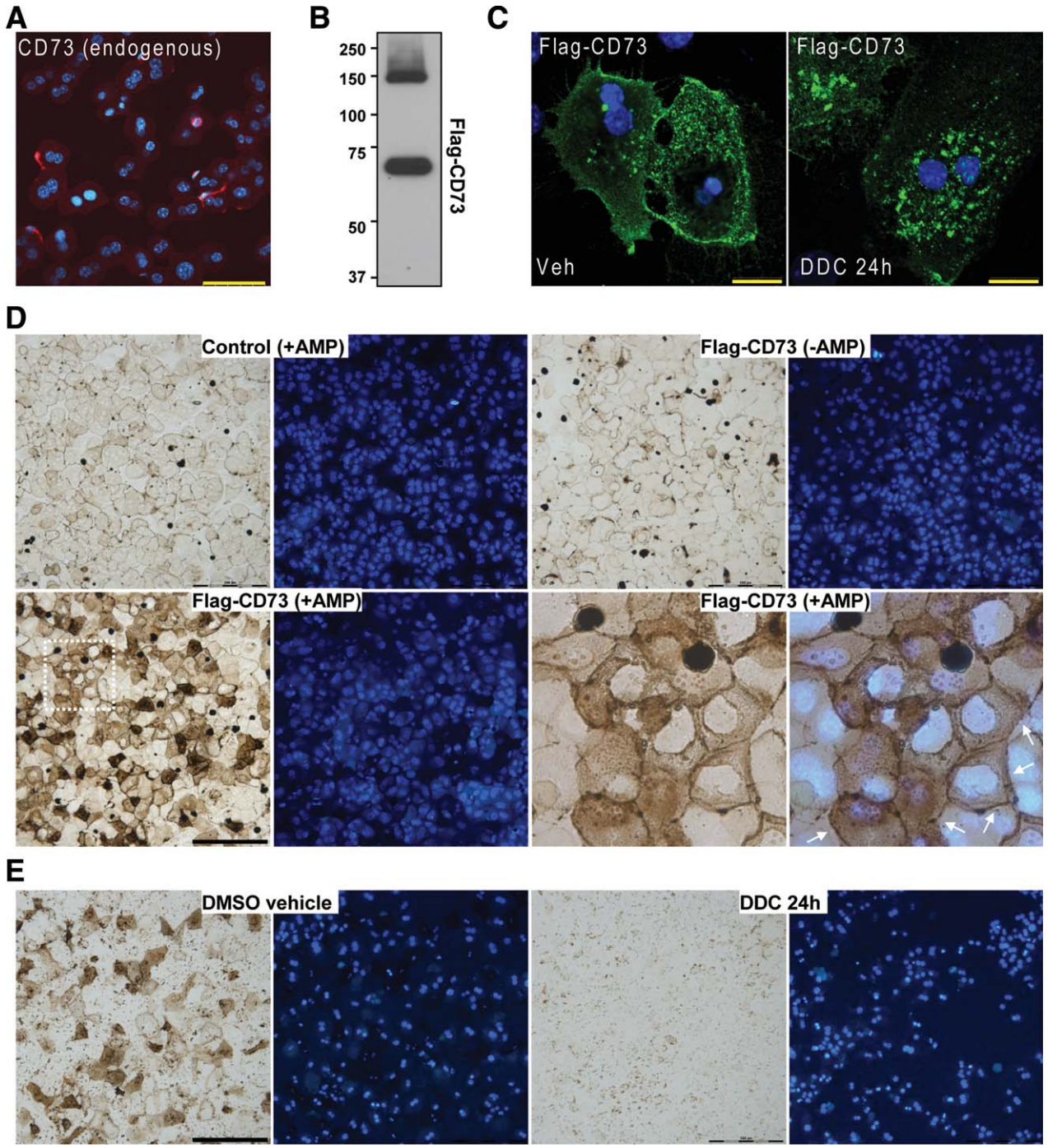

Fig. 3. DDC modulates CD73 localization in primary mouse hepatocytes. (A) IF detection of endogenous CD73 protein (red), which is largely lost in freshly isolated hepatocytes (1 hour postisolation). Blue = DAPI-stained nuclei; scale bar = 50 μm. (B) Flag immunobloting detection of CD73 monomer (68 kD) and dimer (~140 kD) after expression of flag-tagged mouse CD73 in hepatocytes . (C) Loss of plasma membrane CD73 (green) after DDC treatment (100 μM for 24 hours) of primary hepatocytes. Blue = DAPI-stained nuclei; scale bars = 20 μm. (D) AMPase activity in control and Flag-CD73-transfected hepatocytes showing that overexpressed CD73 is enzymatically active. Blue = DAPI-stained nuclei. Lower right two panels represent a magnified view of the area demarcated by a white dotted line in the lower left panel. Arrows point out plasma membrane-associated AMPase activity. Scale bar = 200 μm. (E) AMPase activity in Flag-CD73-transfected hepatocytes that were treated with dimethyl sulfoxide (DMSO) vehicle or 100 μM DDC for 24 hours showing DDC-induced inhibition of CD73 enzymatic activity. Blue = DAPI-stained nuclei; scale bar = 200 μm.

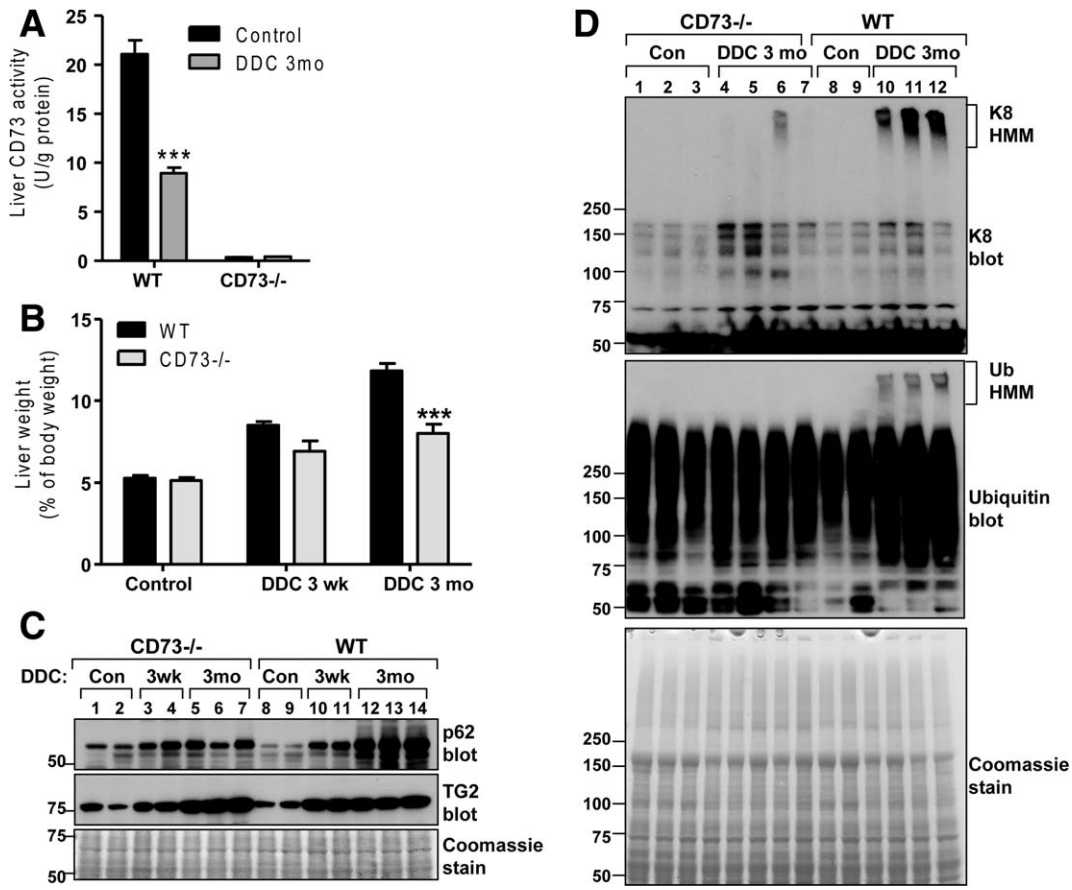

Fig. 4. Comparison of biochemical markers of liver injury in DDC-treated WT and CD73$^{-/-}$ mice. (A) Measurement of CD73 activity in livers from untreated (control) and DDC-treated (3 months) WT and CD73$^{-/-}$ mice. (B) CD73$^{-/-}$ mice had lower liver/body-weight ratio after 3 months of DDC treatment, relative to WT mice. ***$P < 0.001$; two-way analysis of variance. (C) Immunoblotting analysis of p62 (MDB component) and TG2 in total liver lysates of WT and CD73$^{-/-}$ mice. (D) Immunoblottings of K8 and ubiquitin (Ub) from total liver lysates of WT and CD73$^{-/-}$ mice showing the presence of high-molecular-mass (HMM) K8 and Ub complexes in WT, but not CD73$^{-/-}$, mice after DDC treatment for 3 months.

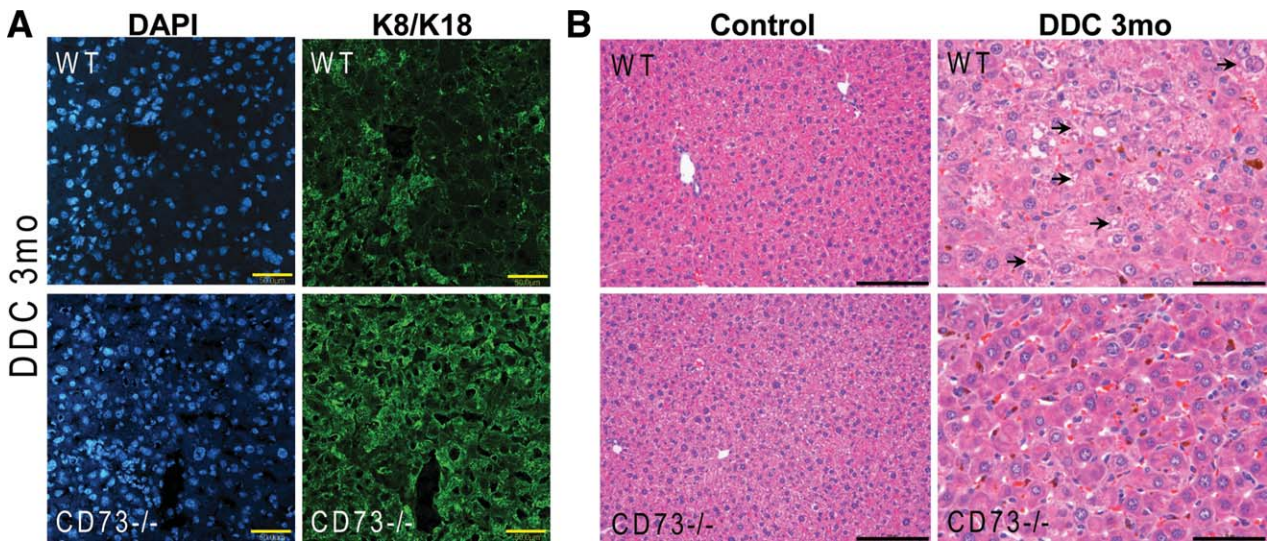

Fig. 5. Comparison of DDC-induced liver injury in WT and CD73$^{-/-}$ mice. (A) Double IF staining for K8/K18 (green) and DAPI nuclei (blue) shows that the K8/K18 filament network is preserved in CD73$^{-/-}$ mouse livers relative to WT livers after DDC treatment for 3 months. Scale bars = 50 μm. (B) H&E staining shows more prominent steatosis, cellular ballooning, and MDBs (marked by arrows) in WT, relative to CD73$^{-/-}$, mice. Results are representative from 3 separate WT and 4 CD73$^{-/-}$ mouse livers. Scale bars = 100 μm (control) and 50 μm (DDC).

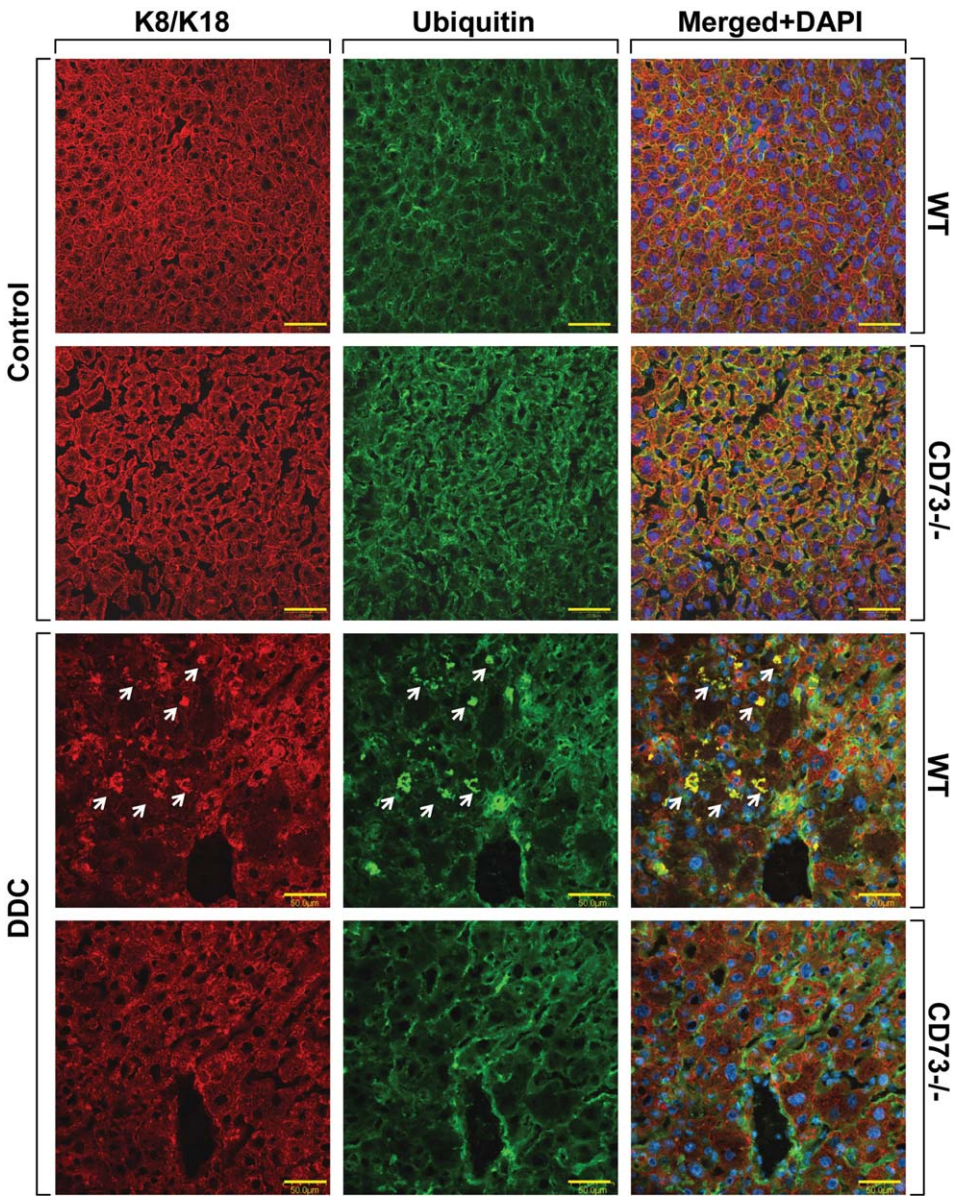

Fig. 6. IF analysis of MDBs in livers from WT and CD73$^{-/-}$ mice. Freshly frozen tissue sections from control and DDC-treated (3 months) WT and C57BL mice were stained with Abs against K8/K18 (red) and ubiquitin (green). MDBs (marked by arrows) are only present in WT livers after DDC treatment. Shown are representative results from three separate WT and four CD73$^{-/-}$ mouse livers. Scale bars = 50 μm.

we identified the ectonucleotidase, CD73, as a promoting factor for MDB formation in mice.

Our findings coincide with recent studies highlighting a role for CD73 in liver pathophysiology. In mouse models of liver fibrosis triggered by thioacetamide or CCl_4, the absence of CD73 is protective.[19] On the other hand, it was previously shown that CCl_4-induced liver damage and concanavalin A-induced liver injury and release of proinflammatory cytokines were exacerbated in adenosine receptor 2A-deficient mice.[27] In further support of a profibrogenic role of CD73 in mouse liver, CD73 is transcriptionally up-regulated in activated hepatic stellate cells during myofibroblast differentiation.[28] However, in our present findings, we show that CD73 mRNA is dramatically decreased in fibrotic human livers (regardless of etiology or fibrosis severity). Potential CD73 expression changes during various stages of human disease progression that are not always reflected in experimental models and the presence of other factors, such as inflammation and steatosis, may be behind these observations. CD73 activity and adenosine receptor activation have also been implicated in ethanol-induced hepatic steatosis in mice.[18] Specifically, CD73$^{-/-}$ mice are protected from developing fatty liver.[18] Given that MDBs are commonly observed in steatohepatitis,[1,14] our findings that CD73$^{-/-}$ mice have less steatosis and are protected from MDBs align with these previous studies.

Although our data demonstrate a role for CD73 in MDB formation, the use of the full-body CD73 KO does not allow us to discern whether this involves a hepatocyte-intrinsic mechanism or is influenced by CD73 on other cells (e.g., immune or endothelial). CD73 is expressed on multiple cell types, including leukocytes, myofibroblasts, endothelial, and epithelial cells.[16,28] A previous study using ferritin immunoelectron microscopy compared the expression and plasma membrane distribution of CD73 in endothelial cells (ECs) and hepatocytes in rat liver.[29] This study found that the bile canalicular surface of hepatocytes had approximately 4-fold higher density of CD73, relative to the sinusoidal surface,[29] which might be expected for a glycosylphosphatidylinositol-anchored protein.[17] Relative to hepatocytes, ECs were estimated to have approximately 60% fewer CD73 molecules.[29]

Given the direct effects of DDC on CD73 localization, we posit that at least some of the *in vivo* findings are directly attributable to hepatocyte CD73. A previous study estimated that only 48% of hepatocyte CD73 activity is on the cell surface, in contrast to 75%-79% of the CD73 activity in adipocytes and lymphocyte being accounted for by the cell-surface-localized enzyme.[30] The intracellular CD73 fraction is membrane associated and enzymatically active, but latent (available to substrate only upon cell breakage), and the exact organelle compartments that host intracellular CD73 are unclear.[30] There is dynamic cycling of the intracellular CD73 pool to the plasma membrane, but only a small fraction (~3%) of it is thought to be lysosomal.[31] If and how the cellular distribution of CD73 in hepatocytes affects intracellular protein aggregation remains to be investigated.

Protein aggregation is a common disease mechanism for multiple organ pathologies and is characterized by protein misfolding and proteasomal inhibition. Uncovering molecular modulators that regulate protein aggregation will not only provide insight into potential tissue- and cell-type-specific pathways, but may also shed light on individual susceptibility to intracellular inclusions. To our knowledge, this is the first report that alterations in purine metabolism and CD73 activity act as modulators of protein aggregation. Given the widespread expression and functional significance of CD73,[16] these findings may hold true in other tissues and cell types. Furthermore, our findings point to dramatic differences in CD73 mRNA and protein levels between two different mouse strains. It would be relevant to determine whether differences in CD73 expression are also present in genetically diverse human populations and whether CD73 contributes to human MDB formation or susceptibility to liver disease.

Acknowledgment: The authors thank Dr. Linda Thompson for providing the $CD73^{-/-}$ mice and for her critical reading of the manuscript.

References

1. Zatloukal K, French SW, Stumptner C, Strnad P, Harada M, Toivola DM, et al. From Mallory to Mallory-Denk bodies: what, how, and why? Exp Cell Res 2007;313:2033-2049.
2. Zatloukal K, Fesus L, Denk H, Tarcsa E, Spurej G, Bock G. High amount of epsilon-(gamma-glutamyl)lysine cross-links in Mallory bodies. Lab Invest 1992;66:774-777.
3. Strnad P, Harada M, Siegel M, Terkeltaub RA, Graham RM, Khosla C, Omary MB. Transglutaminase 2 regulates mallory body inclusion formation and injury-associated liver enlargement. Gastroenterology 2007;132:1515-1526.
4. Lackner C, Gogg-Kamerer M, Zatloukal K, Stumptner C, Brunt EM, Denk H. Ballooned hepatocytes in steatohepatitis: the value of keratin immunohistochemistry for diagnosis. J Hepatol 2008;48:821-828.
5. Kleiner DE, Brunt EM. Nonalcoholic fatty liver disease: pathologic patterns and biopsy evaluation in clinical research. Semin Liver Dis 2012;32:3-13.
6. Cortez-Pinto H, Baptista A, Camilo ME, De Moura MC. Nonalcoholic steatohepatitis—a long-term follow-up study: comparison with alcoholic hepatitis in ambulatory and hospitalized patients. Dig Dis Sci 2003;48:1909-1913.
7. Gramlich T, Kleiner DE, McCullough AJ, Matteoni CA, Boparai N, Younossi ZM. Pathologic features associated with fibrosis in nonalcoholic fatty liver disease. Hum Pathol 2004;35:196-199.
8. Molnar A, Haybaeck J, Lackner C, Strnad P. The cytoskeleton in nonalcoholic steatohepatitis: 100 years old but still youthful. Expert Rev Gastroenterol Hepatol 2011;5:167-177.
9. Gerber MA, Orr W, Denk H, Schaffner F, Popper H. Hepatocellular hyalin in cholestasis and cirrhosis: its diagnostic significance. Gastroenterology 1973;64:89-98.
10. Fleming KA, McGee JO. Alcohol induced liver disease. J Clin Pathol 1984;37:721-733.
11. Rakoski MO, Brown MB, Fontana RJ, Bonkovsky HL, Brunt EM, Goodman ZD, et al. Mallory-Denk bodies are associated with outcomes and histologic features in patients with chronic hepatitis C. Clin Gastroenterol Hepatol 2011;9:902-909.e1.
12. Hanada S, Strnad P, Brunt EM, Omary MB. The genetic background modulates susceptibility to mouse liver Mallory-Denk body formation and liver injury. HEPATOLOGY 2008;48:943-952.
13. Omary MB, Ku NO, Strnad P, Hanada S. Toward unraveling the complexity of simple epithelial keratins in human disease. J Clin Invest 2009;119:1794-1805.
14. Strnad P, Zatloukal K, Stumptner C, Kulaksiz H, Denk H. Mallory-Denk-bodies: lessons from keratin-containing hepatic inclusion bodies. Biochim Biophys Acta 2008;1782:764-774.
15. Snider NT, Weerasinghe SV, Singla A, Leonard JM, Hanada S, Andrews PC, et al. Energy determinants GAPDH and NDPK act as genetic modifiers for hepatocyte inclusion formation. J Cell Biol 2011;195:217-229.
16. Colgan SP, Eltzschig HK, Eckle T, Thompson LF. Physiological roles for ecto-5′-nucleotidase (CD73). Purinergic Signal 2006;2:351-360.
17. Resta R, Yamashita Y, Thompson LF. Ecto-enzyme and signaling functions of lymphocyte CD73. Immunol Rev 1998;161:95-109.
18. Peng Z, Borea PA, Varani K, Wilder T, Yee H, Chiriboga L, et al. Adenosine signaling contributes to ethanol-induced fatty liver in mice. J Clin Invest 2009;119:582-594.
19. Peng Z, Fernandez P, Wilder T, Yee H, Chiriboga L, Chan ES, Cronstein BN. Ecto-5′-nucleotidase (CD73)-mediated extracellular adenosine production plays a critical role in hepatic fibrosis. FASEB J 2008;22:2263-2272.
20. Ku NO, Michie S, Oshima RG, Omary MB. Chronic hepatitis, hepatocyte fragility, and increased soluble phosphoglycokeratins in transgenic mice expressing a keratin 18 conserved arginine mutant. J Cell Biol 1995;131:1303-1314.

21. Thompson LF, Eltzschig HK, Ibla JC, Van De Wiele CJ, Resta R, Morote-Garcia JC, Colgan SP. Crucial role for ecto-5′-nucleotidase (CD73) in vascular leakage during hypoxia. J Exp Med 2004;200: 1395-1405.
22. Frederiks WM, Marx F. A quantitative histochemical study of 5′-nucleotidase activity in rat liver using the lead salt method and polyvinyl alcohol. Histochem J 1988;20:207-214.
23. Bieche I, Asselah T, Laurendeau I, Vidaud D, Degot C, Paradis V, et al. Molecular profiling of early stage liver fibrosis in patients with chronic hepatitis C virus infection. Virology 2005;332:130-144.
24. Greco D, Kotronen A, Westerbacka J, Puig O, Arkkila P, Kiviluoto T, et al. Gene expression in human NAFLD. Am J Physiol Gastrointest Liver Physiol 2008;294:G1281-G1287.
25. Knapp K, Zebisch M, Pippel J, El-Tayeb A, Muller CE, Strater N. Crystal structure of the human ecto-5′-nucleotidase (CD73): insights into the regulation of purinergic signaling. Structure 2012;20:2161-2173.
26. Hanada S, Snider NT, Brunt EM, Hollenberg PF, Omary MB. Gender dimorphic formation of mouse Mallory-Denk bodies and the role of xenobiotic metabolism and oxidative stress. Gastroenterology 2010;138:1607-1617.
27. Ohta A, Sitkovsky M. Role of G-protein-coupled adenosine receptors in downregulation of inflammation and protection from tissue damage. Nature 2001;414:916-920.
28. Fausther M, Sheung N, Saiman Y, Bansal MB, Dranoff JA. Activated hepatic stellate cells upregulate transcription of ecto-5′-nucleotidase/CD73 via specific SP1 and SMAD promoter elements. Am J Physiol Gastrointest Liver Physiol 2012;303:G904-G914.
29. Matsuura S, Eto S, Kato K, Tashiro Y. Ferritin immunoelectron microscopic localization of 5′-nucleotidase on rat liver cell surface. J Cell Biol 1984;99:166-173.
30. Stanley KK, Edwards MR, Luzio JP. Subcellular distribution and movement of 5′-nucleotidase in rat cells. Biochem J 1980;186:59-69.
31. Maguire GA, Luzio JP. The presence and orientation of ecto-5′-nucleotidase in rat liver lysosomes. FEBS Lett 1985;180:122-126.